ELSEVIER

Electrical Power and Energy Systems 22 (2000) 247–258

ELECTRICAL POWER & ENERGY SYSTEMS

www.elsevier.com/locate/ijepes

Simulated annealing based approach to PSS and FACTS based stabilizer tuning

M.A. Abido*

Electrical Engineering Department, King Fahd University of Petroleum and Minerals, Dhahran 31261, Saudi Arabia

Abstract

A simulated annealing (SA) based approach to power system stabilizer (PSS) and FACTS based stabilizer tuning has been investigated in this paper. The design problem of PSS and FACTS based stabilizer is formulated as an optimization problem. An eigenvalue-based objective function to increase the system damping is proposed. Then, SA algorithm is employed to search for optimal stabilizer parameters. Different control schemes have been proposed and tested on a weakly connected power system with different disturbances, loading conditions, and parameter variations. Nonlinear simulation results show the potential of SA algorithm to the tuning problem of PSS and FACTS based stabilizer. Effectiveness and robustness of the proposed control schemes over a wide range of loading conditions and system parameter variations have been demonstrated. It was also observed that the SPS controller provides most of the damping and improves greatly the voltage profile of the system under severe disturbances. © 2000 Elsevier Science Ltd. All rights reserved.

Keywords: Power system stabilizer; FACTS based stabilizer; Simulated annealing algorithm

1. Introduction

Due to increasing complexity of electrical power systems, there has been increasing interest in the stabilization of such systems. In the past two decades, the utilization of supplementary excitation control signals for improving the dynamic stability of power systems and damping out the low frequency oscillations has received much attention [1–14]. Nowadays, the conventional power system stabilizer (CPSS)—a fixed parameters lead–lag compensator—is widely used by power system utilities [4]. In addition, several approaches based on modern control theory have been applied to PSS design problem. These include optimal control, adaptive control, variable structure control, and intelligent control [10–14].

Although PSSs extend the power system stability limit by enhancing the system damping, they suffer a drawback of being liable to cause great variations in the voltage profile and they may even result in leading power factor operation and losing system stability under severe disturbances [15–17].

The recent advances in power electronics have led to the development of the flexible alternating current transmission systems (FACTS). FACTS are designed to overcome the limitations of the present mechanically controlled power systems and enhance power system stability by using reliable and high-speed electronic devices. One of the promising FACTS devices is the static phase shifter (SPS). The effectiveness of the SPS in improving power system stability has been investigated in several studies with promising results [18–27]. This provides an alternative choice to PSSs in suppressing power system oscillations.

A considerable attention has been directed to realization of various SPS schemes [18]. However, a relatively little work in SPS control aspects has been reported in the literature. Baker et al. [20] developed a control algorithm for SPS using stochastic optimal control theory. Edris [22] proposed a simple control algorithm based on equal area criterion. Recently, Jiang et al. [24] proposed an SPS control technique based on nonlinear variable structure control theory. In their control scheme the phase shift angle is determined as a nonlinear function of rotor angle and speed. However, in real life power system with a large number of generators, the rotor angle of a single generator measured with respect to the system reference will not be very meaningful. Tan and Wang [25] proposed a direct feedback linearization technique to linearize and decouple the power system model to design the excitation and SPS controllers.

Despite the potential of modern control techniques with different structures, power system utilities still prefer a conventional lead–lag controller structure [4–6]. The reasons behind that might be the ease of on-line tuning and the lack of assurance of the stability related to some

* Tel.: +966-3-8604379; fax: +966-3-8603535.
E-mail address: mabido@kfupm.edu.sa (M.A. Abido).

0142-0615/00/$ - see front matter © 2000 Elsevier Science Ltd. All rights reserved.
PII: S0142-0615(99)00055-1

Nomenclature

D	damping constant of the generator
E_{fd}	field voltage
E'_q	transient EMF in q-axis of the generator
i_d	d-axis component of the armature current
i_q	q-axis component of the armature current
K_A	gain of the excitation system
K_s	gain of the SPS
P_m	mechanical input power of the generator
P_e	electrical output power of the generator
T'_{do}	open circuit field time constant
T_A	time constant of the excitation system
T_s	time constant of the SPS
u_{PSS}	output signal of the PSS
u_{SPS}	output signal of the SPS controller
v	terminal voltage of the generator
v_d	d-axis component of the terminal voltage
v_q	q-axis component of the terminal voltage
v_{SPS}	injected voltage by SPS
V_{ref}	reference voltage
x_d	d-axis reactance of the generator
x'_d	d-axis transient reactance of the generator
x_q	q-axis reactance of the generator
Y_L	local load admittance, $Y_L = g + jb$
Z	transmission line impedance, $Z = R + jX$
Greeks	
δ	rotor angle of the generator
ρ	derivative operator d/dt
ω	speed of the generator
Φ_{ref}	reference angle
Φ	phase shift angle of the SPS

adaptive or variable structure techniques. It is shown that the appropriate selection of conventional lead-lag stabilizer parameters results in effective damping to low frequency oscillations [4,6]. A gradient procedure for optimization of PSS parameters is presented in [28]. The optimization process requires computations of sensitivity factors and eigenvectors at each iteration. This gives rise to heavy computational burden and slow convergence. In addition, the search process is susceptible to be trapped in local minima and the solution obtained will not be optimal. To overcome the shortcomings of the previous methods and to avoid computations of sensitivity factors and eigenvectors, SA based approach to PSS design is proposed.

In the last few years, simulated annealing (SA) algorithm [29,30] appeared as a promising heuristic algorithm for handling the combinatorial optimization problems. It has been theoretically proved that the SA algorithm converges to the optimum solution. The SA algorithm is robust i.e. the final solution quality does not strongly depend on the choice of the initial solution. Therefore, the algorithm can be used to improve the solution of other methods. Another strong feature of SA algorithm is that a complicated mathematical model is not needed and the constraints can be easily incorporated [29]. Unlike the gradient-descent techniques, SA is a derivative-free optimization algorithm and no sensitivity analysis is required to evaluate the objective function. This feature simplifies the constraints imposed on the objective function considered.

In this paper, design of PSS and SPS controller using SA algorithm is investigated. In addition, an assessment of the effects of PSS and SPS control when applied independently and also through coordinated application has been carried out. The controller design problem is formulated as an optimization problem. Then, SA algorithm is employed to solve this problem with the aim of getting the optimal or near optimal settings of the controller parameters. Different control schemes have been proposed and tested on a weakly connected power system. Based on eigenvalue analysis and simulation results, it was observed that the proposed control schemes provide good damping of electromechanical modes of oscillations, enhance power system stability, and improve the system voltage profile.

2. Linearized power system model

In this study, a single machine infinite bus system with an SPS shown in Fig. 1 is considered. The SPS has a ratio of $1:1\angle -\Phi$. In this case, the real power flow can be described as

$$P_e = \frac{E'_q v_b}{X}\sin(\delta - \Phi) \tag{1}$$

Hence, the real power flow can be regulated to mitigate the low frequency oscillations and enhance power system transient stability by controlling either the internal voltage E'_q or the angle Φ. While the power system stabilizer can control E'_q through the generator excitation system, the static phase shifter can control the relative phase angle between the system voltages by adjusting the angle Φ.

The generator is represented by the third-order model comprising of the electromechanical swing equation and the generator internal voltage equation. The swing equation is divided to the following equations

$$\rho\delta = \omega_b(\omega - 1) \tag{2}$$

$$\rho\omega = (P_m - P_e - D(\omega - 1))/M \tag{3}$$

P_m is assumed to be constant and P_e can be expressed as

$$P_e = v_d i_d + v_q i_q \tag{4}$$

The internal voltage, E'_q, equation is

$$\rho E'_q = (E_{fd} - (x_d - x'_d)i_d - E'_q)/T'_{do} \tag{5}$$

The IEEE Type-ST1 excitation system shown in Fig. 2 is considered in this study. It can be described as

$$\rho E_{fd} = (K_A(V_{ref} - v + u_{PSS}) - E_{fd})/T_A \tag{6}$$

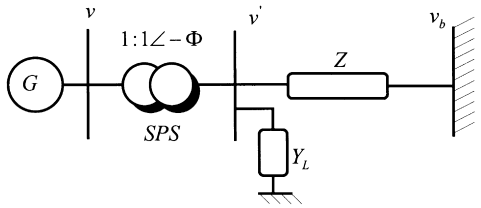

Fig. 1. Single machine infinite bus system with an SPS.

where;

$$v = (v_d^2 + v_q^2)^{1/2} \tag{7}$$

and;

$$v_d = x_q i_q \tag{8}$$

$$v_q = E'_q - x'_d i_d \tag{9}$$

Fig. 3 illustrates the block diagram of an SPS controller. The phase shift angle of the SPS, Φ, is expressed as

$$\rho\Phi = (K_s(\Phi_{ref} - u_{SPS}) - \Phi)/T_s \tag{10}$$

In the design of PSS and SPS damping controller, the linearized incremental model around a nominal operating point is usually employed [1–3]. Linearizing the above model yield the following linearized power system model, see Appendix A,

$$\begin{bmatrix} \rho\Delta\delta \\ \rho\Delta\omega \\ \rho\Delta E'_q \\ \rho\Delta E_{fd} \end{bmatrix} = \begin{bmatrix} 0 & 377 & 0 & 0 \\ -\frac{K_1}{M} & -\frac{D}{M} & -\frac{K_2}{M} & 0 \\ -\frac{K_4}{T'_{do}} & 0 & -\frac{K_3}{T'_{do}} & \frac{1}{T'_{do}} \\ -\frac{K_A K_5}{T_A} & 0 & -\frac{K_A K_6}{T_A} & -\frac{1}{T_A} \end{bmatrix} \times \begin{bmatrix} \Delta\delta \\ \Delta\omega \\ \Delta E'_q \\ \Delta E_{fd} \end{bmatrix} + \begin{bmatrix} 0 & 0 \\ 0 & -\frac{K_p}{M} \\ 0 & -\frac{K_q}{T'_{do}} \\ \frac{K_A}{T_A} & -\frac{K_A K_v}{T_A} \end{bmatrix} \begin{bmatrix} u_{PSS} \\ \Delta\Phi \end{bmatrix} \tag{11}$$

In short, the linearized system model can be written as

$$\rho X = AX + BU \tag{12}$$

Here, the state vector X is $[\Delta\delta, \Delta\omega, \Delta E'_q, \Delta E_{fd}]^T$ and the control vector U is $[u_{PSS}, \Delta\Phi]^T$.

Fig. 4 illustrates the block diagram of the linearized power system model. The expressions of constants K_1–K_6, K_p, K_q, and K_v are given in Appendix A.

3. Proposed control schemes

3.1. PSS and SPS controller structure

A conventional lead–lag controller structure for both PSS and SPS as shown in Figs. 2 and 3 is considered in this study. The stabilizing signals of the proposed PSS and SPS controller can be expressed as

$$u_{PSS} = K_{PSS} \frac{sT_w}{1 + sT_w} \left(\frac{1 + sT_{1PSS}}{1 + sT_{2PSS}} \right) \left(\frac{1 + sT_{3PSS}}{1 + sT_{4PSS}} \right) \Delta\omega \tag{13}$$

$$u_{SPS} = K_{SPS} \frac{sT_w}{1 + sT_w} \left(\frac{1 + sT_{1SPS}}{1 + sT_{2SPS}} \right) \left(\frac{1 + sT_{3SPS}}{1 + sT_{4SPS}} \right) \Delta\omega \tag{14}$$

In this structure, the washout time constant T_w and the time constants T_{2PSS}, T_{4PSS}, T_{2SPS}, and T_{4SPS} are usually prespecified. In this study, $T_w = 5$ s and $T_{2PSS} = T_{4PSS} = T_{2SPS} = T_{4SPS} = 0.1$ s. The controller gains, K_{PSS} and K_{SPS}, and time constants, T_{1PSS}, T_{3PSS}, T_{1SPS} and T_{3SPS} remain to be determined. It is seen [31] that the effort of phase shifter is to change the mutual admittance between the fault location and the generator bus. Therefore, the best location of the SPS is at the generator terminal as it gives the greatest change of electrical distance between the generator and the disturbance point. Hence, the speed deviation $\Delta\omega$ is available and used as the input signal to both PSS and SPS controller. This makes the proposed controllers easy for on-line implementation.

3.2. Proposed control schemes

To investigate the ability of PSS and SPS controller to damp out the low frequency oscillations associated with the electromechanical modes, the following control schemes are proposed.

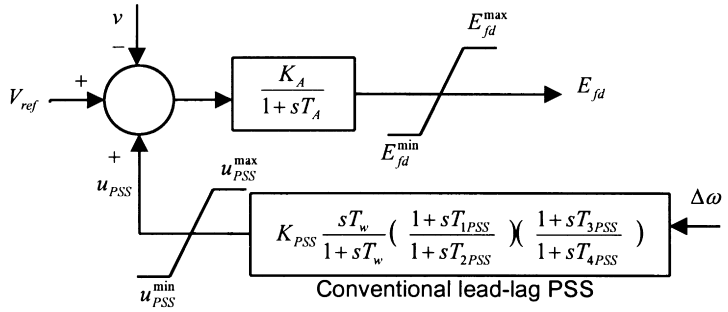

Fig. 2. IEEE Type-ST1 excitation system with conventional lead–lag PSS.

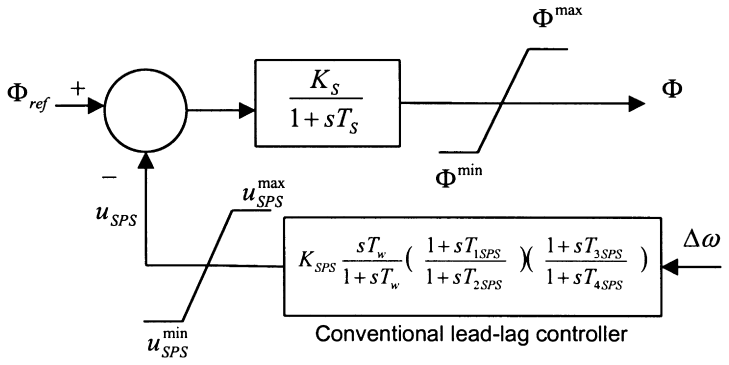

Fig. 3. SPS with conventional lead–lag controller.

- *Scheme (a)* where PSS only is considered. In this case, the tuning parameters are K_{PSS}, T_{1PSS} and T_{3PSS}.
- *Scheme (b)* where SPS controller only is considered. In this case, the tuning parameters are K_{SPS}, T_{1SPS}, and T_{3SPS}.
- *Scheme (c)* where coordinated design of both PSS and SPS controller is considered. In this case, the tuning parameters are K_{PSS}, T_{1PSS}, T_{3PSS}, K_{SPS}, T_{1SPS} and T_{3SPS}.

3.3. PSS and SPS controller design

As far as the electromechanical modes are concerned, the first step in the design process is to identify the eigenvalues of the system matrix A associated with these modes. Participation factors method [32] is used for this purpose. An eigenvalue-based objective function J defined below is proposed.

$$J = \zeta \text{of electromechanical mode} \tag{15}$$

where ζ is the damping ratio. This objective function is proposed to improve the time domain control system specifications such as damping factor, overshoots, and settling time.

The problem constraints are the optimized parameter bounds. Therefore, the design problem can be formulated as the following optimization problem.

$$\text{Maximize } J \tag{16}$$

subject to

$$K_{PSS}^{min} \le K_{PSS} \le K_{PSS}^{max} \tag{17}$$

$$T_{1PSS}^{min} \le T_{1PSS} \le T_{1PSS}^{max} \tag{18}$$

$$T_{3PSS}^{min} \le T_{3PSS} \le T_{3PSS}^{max} \tag{19}$$

$$K_{SPS}^{min} \le K_{SPS} \le K_{SPS}^{max} \tag{20}$$

$$T_{1SPS}^{min} \le T_{1SPS} \le T_{1SPS}^{max} \tag{21}$$

$$T_{3SPS}^{min} \le T_{3SPS} \le T_{3SPS}^{max} \tag{22}$$

The minimum and maximum values of the controller gains are set as 0.1 and 100, respectively [2]. The minimum values of T_{1PSS} and T_{3PSS} are set slightly above the value of T_{2PSS} and T_{4PSS}, respectively to compensate the phase lag

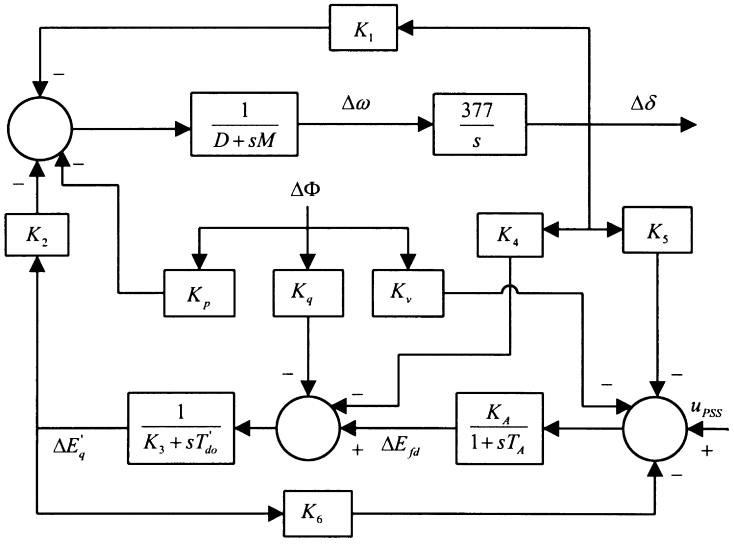

Fig. 4. Block diagram of the linearized power system model.

between u_{PSS} and E'_q [1]. The maximum values of T_{1PSS}, T_{3PSS}, T_{1SPS}, and T_{3SPS} are set to 1.0 s.

The proposed approach employs SA algorithm to solve this optimization problem and search for optimal or near optimal set of the optimized parameters.

4. Simulated annealing algorithm

4.1. Overview

Simulated annealing is an optimization technique that simulates the physical annealing process in the field of combinatorial optimization. Annealing is the physical process of heating up a solid until it melts, followed by slow cooling it down by decreasing the temperature of the environment in steps. At each step, the temperature is maintained constant for a period of time sufficient for the solid to reach thermal equilibrium. At any temperature T, the thermal equilibrium state is characterized by the *Boltzmann distribution*. This distribution gives the probability of the solid being in a state i with energy E_i at temperature T as

$$P_i = k \exp(-E_i/T) \tag{23}$$

where k is a constant.

Metropolis et al. [30] proposed a Monte Carlo method to simulate the process of reaching thermal equilibrium at a fixed value of the temperature T. In this method, a randomly generated perturbation of the current configuration of the solid is applied so that a trial configuration is obtained. Let E_c and E_t denote the energy level of the current and trial configurations, respectively. If $E_t < E_c$, then a lower energy level has been reached, and the trial configuration is accepted and becomes the current configuration. On the other hand, if $E_t \geq E_c$ the trial configuration is accepted as current configuration with probability proportional to $\exp(-\Delta E/T)$, $\Delta E = E_t - E_c$. The process continues until the thermal equilibrium is achieved after a large number of perturbations, where the probability of a configuration approaches Boltzmann distribution.

By gradually decreasing the temperature T and repeating Metropolis simulation, new lower energy levels become achievable. As T approaches *zero* least energy configurations will have a positive probability of occurring.

4.2. SA algorithm

At first, the analogy between a physical annealing process and a combinatorial optimization problem is based on the following [29]:

- Solutions in an optimization problem are equivalent to configurations of a physical system.
- The cost of a solution is equivalent to the energy of a configuration.

In addition, a control parameter C_p is introduced to play the role of the temperature T.

The basic elements of SA are briefly stated and defined as follows:

- *Current, trial and best solutions*, $x_{current}$, x_{trial} and x_{best}: these solutions are sets of the optimized parameter values at any iteration.
- *Acceptance criterion:* at any iteration, the trial solution can be accepted as the current solution if it meets one of the following criteria; (a) $J(x_{trial}) < J(x_{current})$; (b) $J(x_{trial}) > J(x_{current})$ and $\exp(-(J(x_{trial}) - J(x_{current}))/C_p) \geq \text{rand}(0,1)$. Here, rand(0,1) is a random number with domain [0,1] and $J(x_{trial})$ and $J(x_{current})$ are the objective function values associated with x_{trial} and $x_{current}$, respectively. Criterion (b) indicates that the trial solution is not necessarily rejected if its objective function is not as good as that of the current solution with hoping that a much better solution becomes reachable.
- *Acceptance ratio:* at a given value of C_p, an n_1 trial solutions can be randomly generated. Based on the acceptance criterion, an n_2 of these solutions can be accepted. The acceptance ratio is defined as n_2/n_1.
- *Markov chain:* it is defined as a sequence of trial solutions where the probability of the outcome of a given trial solution depends only on the outcome of the previous trial solution. In the SA algorithm, the set of the outcomes is given by the finite set of solutions. The acceptance criteria described above show clearly that the outcome of a trial solution depends only on the outcome of the previous one. Hence, the concept of the Markov chain can be used [29]. The allowable number of transitions at each value of the control parameter C_p represents the length of each chain.
- *Cooling schedule:* it specifies a set of parameters that governs the convergence of the algorithm. This set includes an initial value of control parameter C_{p0}, a decrement function for decreasing the value of C_p, and a finite number of iterations or transitions at each value of C_p, i.e. the length of each homogeneous Markov chain. The initial value of C_p should be large enough to allow virtually all transitions to be accepted. However, this can be achieved by starting off at a small value of C_{p0} and multiplying it with a constant larger than 1, α, i.e. $C_{p0} = \alpha C_{p0}$. This process continues until the acceptance ratio is close to 1. This is equivalent to heating up process in physical systems. The decrement function for decreasing the value of C_p is given by $C_p = \mu C_p$ where μ is a constant smaller than but close to 1. Typical values lie between 0.8 and 0.99 [29]. The acceptance criteria show that at large values of C_p, large deteriorations will be accepted; as C_p decreases, only smaller deteriorations will be accepted and finally, as C_p approaches *zero*, no deteriorations will be accepted at all. This feature, in contrast to gradient-descent and other local search algorithms, avoids trapping in local minima.
- *Equilibrium condition:* it occurs when the current solution does not change for a certain number of iterations at

Table 1
The optimal settings of the controller parameters of the proposed schemes

Prop. scheme (a)			Prop. scheme (b)			Prop. Scheme (c)					
K_{PSS}	T_{1PSS}	T_{3PSS}	K_{SPS}	T_{1SPS}	T_{3SPS}	K_{PSS}	T_{1PSS}	T_{3PSS}	K_{SPS}	T_{1SPS}	T_{3SPS}
20.34	0.120	0.232	96.99	0.080	0.085	40.62	0.150	0.115	8.760	0.944	0.119

a given value of C_p. It can be achieved by generating a large number of transitions at that value of C_p.

- *Stopping criteria:* these are the conditions under which the search process will terminate. In this study, the search will terminate if one of the following criteria is satisfied: (a) the number of Markov chains since the last change of the best solution is greater than a prespecified number; or, (b) the number of Markov chains reaches the maximum allowable number.

The general algorithm of SA can be described in steps as follows:

Step 1: Set the initial value of C_{p0} and randomly generate an initial solution $x_{initial}$ and calculate its objective function. Set this solution as the current solution as well as the best solution, i.e. $x_{initial} = x_{current} = x_{best}$.
Step 2: Randomly generate an n_1 of trial solutions in the neighborhood of the current solution.
Step 3: Check the acceptance criterion of these trial solutions and calculate the acceptance ratio. If acceptance ratio is close to 1 go to Step 4; else set $C_{p0} = \alpha C_{p0}$, $\alpha > 1$, and go back to Step 2.
Step 4: Set the chain counter $k_{ch} = 0$.
Step 5: Generate a trial solution x_{trial}. If x_{trial} satisfies the acceptance criterion set $x_{current} = x_{trial}$, $J(x_{current}) = J(x_{trial})$, and go to Step 6; else go to Step 6.
Step 6: Check the equilibrium condition. If it is satisfied go to Step 7; else go to Step 5.
Step 7: Check the stopping criteria. If one of them is satisfied then stop; else set $k_{ch} = k_{ch} + 1$ and $C_p = \mu C_p$, $\mu < 1$, and go back to Step 5.

5. Application of SA to the proposed control schemes

SA algorithm has been applied to search for optimal settings of the optimized parameters of the proposed control schemes. In our implementation, the search will terminate if the best solution does not change for more than 10 chains or the number of chains reaches 200. Each chain has a length of 300 iterations. The equilibrium condition is satisfied if the current solution does not change for more than 30 iterations. The final settings of the optimized parameters for the proposed schemes are given in Table 1. The convergence rate of the objective function J with the number of iterations is shown in Fig. 5.

It is worth mentioning that the optimization process has been carried out with the system operating at nominal loading condition given in Table 2.

6. Simulation results

To assess the effectiveness and robustness of the proposed control schemes, three different loading conditions given in Table 2 were considered. Moreover, different disturbances and system parameter variations were applied. The performance of the proposed control schemes is compared to that of PSS given in [14] with a transfer

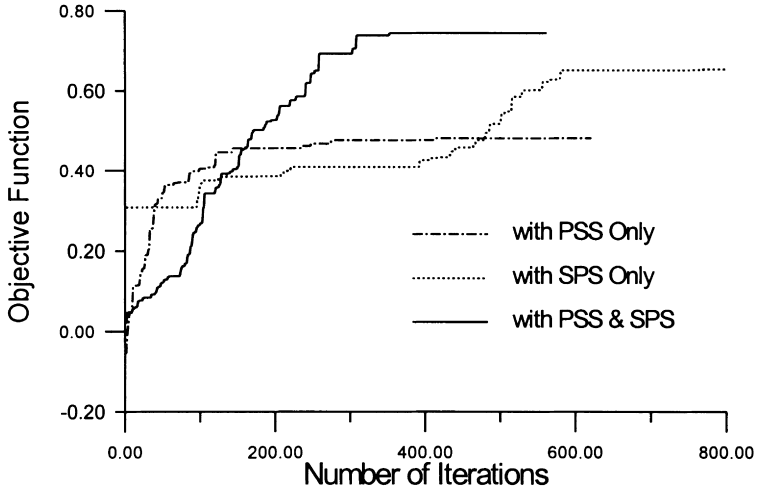

Fig. 5. Objective function variations of the proposed schemes.

Table 2
Loading conditions

Loading	P (pu)	Q (pu)	v (pu)	Φ (°)
Nominal	1.0	0.015	1.05	0.0
Leading PF	0.70	− 0.20	1.05	5.0
Heavy	1.10	0.40	1.05	5.0

function given by

$$u_{\mathrm{PSS}} = 7.091\left(\frac{5s}{1+5s}\right)\left(\frac{1+0.685s}{1+0.1s}\right)\Delta\omega \tag{24}$$

It is worth mentioning that all the time domain simulations were carried out using the nonlinear power system model. The system data is given in Appendix B.

6.1. Nominal loading

At this loading condition, the system eigenvalues with and without the proposed control schemes are given in Table 3. It is shown that the open loop system is unstable and the CPSS [14] stabilizes the system with a damping ratio ζ of electromechanical mode of 0.254. The corresponding damping ratios of the proposed schemes (a)–(c) are 0.481, 0.656 and 0.744, respectively. It is quite clear that the proposed control schemes enhance greatly the damping of electromechanical mode of oscillation. However, better damping characteristics can be achieved with proper coordinated design of PSS and SPS controller as shown in proposed scheme (c).

Two different disturbances were applied to assess the effectiveness of the proposed control schemes to enhance system damping. These disturbances are as follows.

6.1.1. Fault test

The behavior of the proposed control schemes under transient conditions was verified by applying a three-phase fault at the infinite bus at $t = 1$ s. The fault duration was 0.1 s. The system response is shown in Figs. 6 and 7. It can be seen from Fig. 6 that the first swing in the torque angle is significantly suppressed with the proposed schemes (b) and (c). This means that SPS outperforms PSS in damping of first swing and increasing of stability margin. This positive effect can be attributed to the faster response of the SPS. In Fig. 7, the voltage profile is greatly improved with the proposed scheme (b). This confirms that PSS degrades the voltage profile under severe disturbances.

6.1.2. Parameter variation test

To verify the robustness of the proposed schemes to system parameter variation, the system inertia has been reduced by 25% of its nominal value while a 25% pulse increase in the input torque has been applied from $t = 1.0$ to $t = 4.0$ s. The system response is shown in Figs. 8 and 9. The simulation results show that the system response is greatly improved with the proposed schemes. It can be seen that CPSS fails to stabilize the system under this disturbance. The results also demonstrate the robustness of the proposed schemes with system parameter variations. This can be attributed to the optimal selection of the parameter settings of the proposed control schemes. It can be concluded that the performance of damping controllers can be greatly improved when they are optimally designed.

6.2. Leading PF loading

It may become necessary to operate the generator at a leading power factor. In this case, the stability margin is reduced and it becomes important to test the proposed control schemes under this situation. A three-phase fault test has been applied at the infinite bus for 0.1 s. The system response is shown in Figs. 10 and 11. It is shown that the system damping characteristics are significantly enhanced with the proposed control schemes (b) and (c).

6.3. Heavy loading

A three-phase fault disturbance at the infinite bus for 0.05 s was applied. The results are shown in Figs. 12 and 13. It can be seen that the proposed schemes (b) and (c) suppress the first swing in torque angle and extend the system stability limit. In addition, the voltage profile is greatly improved with the proposed scheme (b) in terms of overshoots and settling time. The reason behind this is the faster response of SPS compared to that of PSS. It can be concluded that PSS degrades the terminal voltage response, particularly, under severe disturbances and heavy loading levels.

Table 3
System eigenvalues with and without control

No control	PSS [14]	Prop. scheme (a)	Prop. scheme (b)	Prop. scheme (c)
$+0.295 \pm j4.960$[a]	$-1.157 \pm j4.397$[a]	$-2.795 \pm j5.056$[a]	$-3.221 \pm j3.703$[a]	$-4.009 \pm j3.541$[a]
$-10.393 \pm j3.284$	$-4.602 \pm j7.408$	$-3.500 \pm j6.380$	$-6.628 \pm j7.607$	$-6.260 \pm j5.618$
–	$-0.201, -18.677$	$-0.205, -19.14$	$-11.187 \pm j0.933$	$-10.00 \pm j0.005$
–	–	-8.466	$-0.210, -18.115$	$-15.19 \pm j8.077$
–	–	–	–	$-9.23, -0.21, -0.2$

[a] Eigenvalues associated with the electromechanical mode.

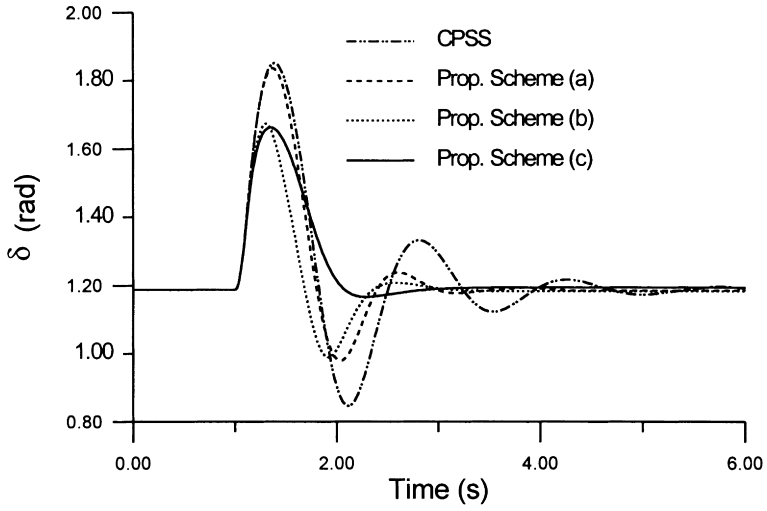

Fig. 6. δ response to the fault test with nominal loading.

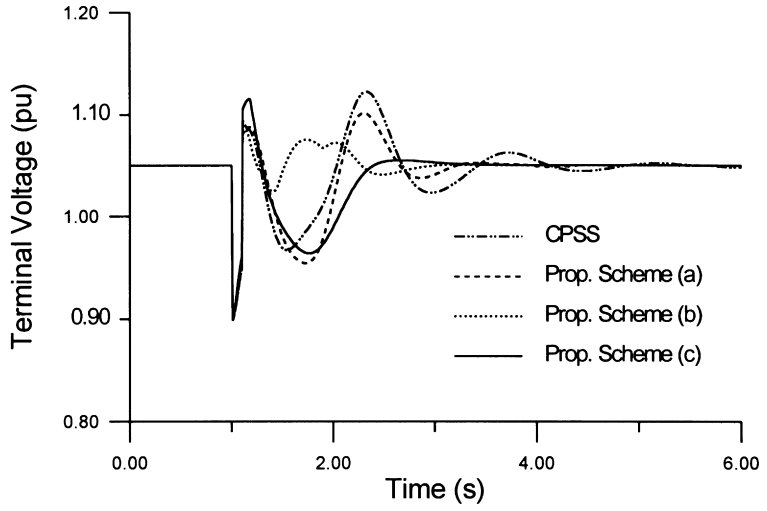

Fig. 7. Terminal voltage response to the fault test with nominal loading.

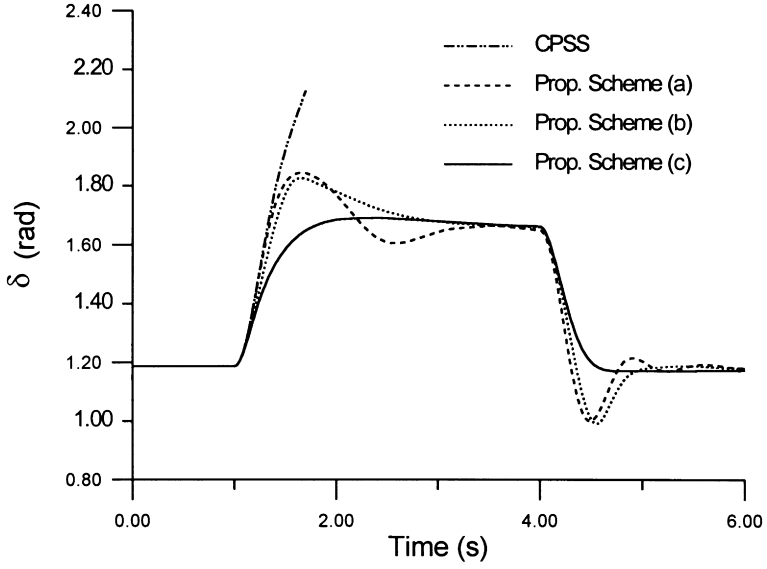

Fig. 8. δ response to the parameter variation test with nominal loading.

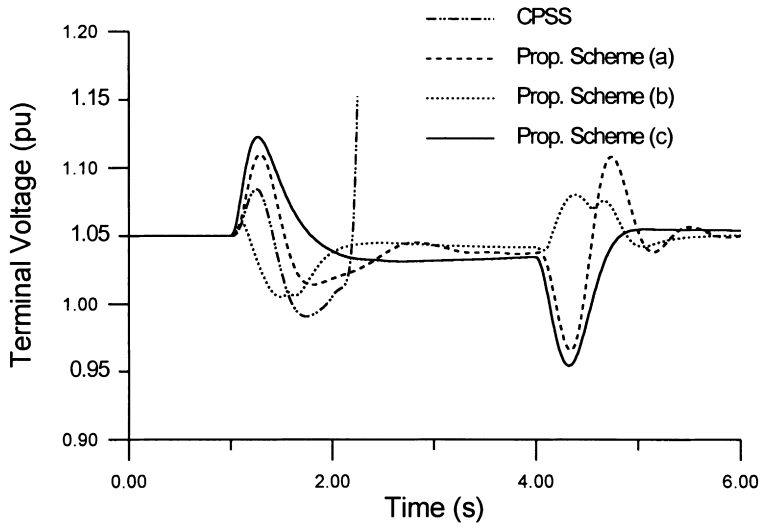

Fig. 9. Terminal voltage response to the parameter variation test with nominal loading.

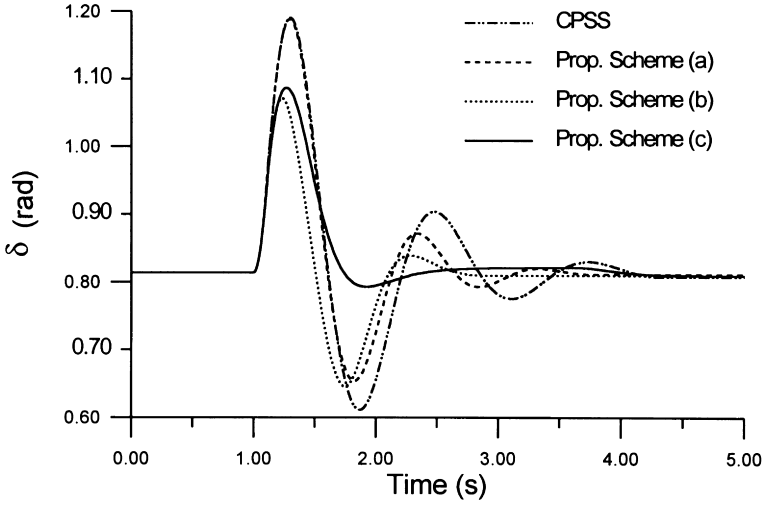

Fig. 10. δ response to the fault test with leading PF loading.

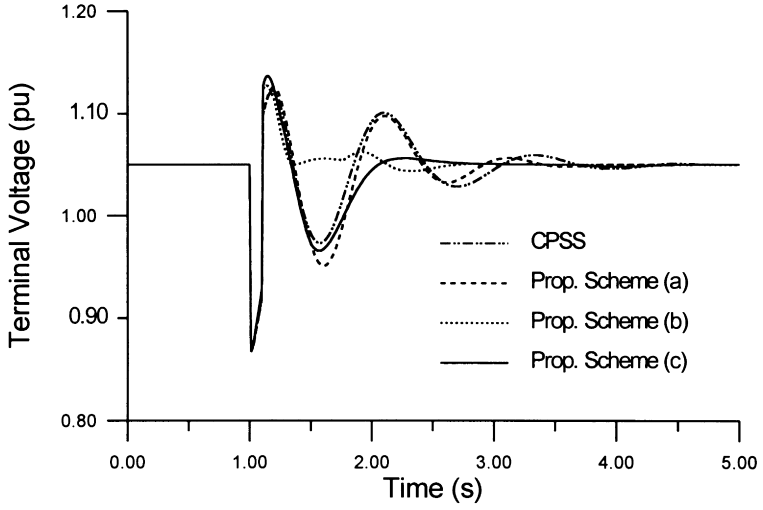

Fig. 11. Terminal voltage response to the fault test with leading PF loading.

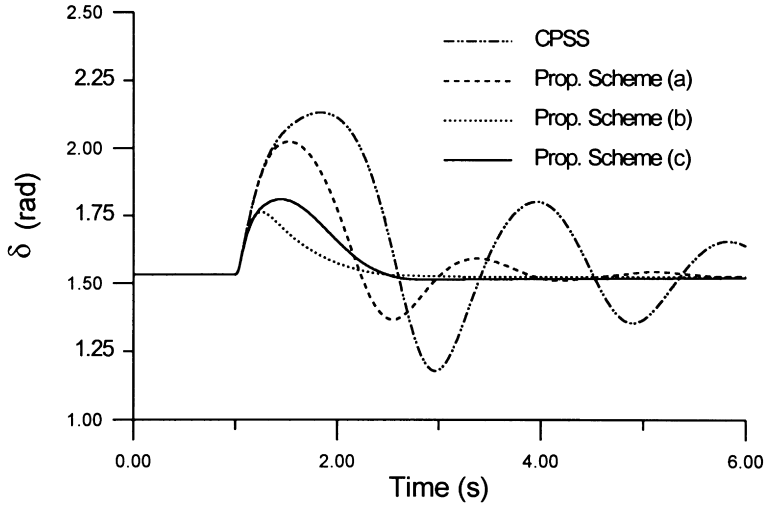

Fig. 12. δ response to the fault test with heavy loading.

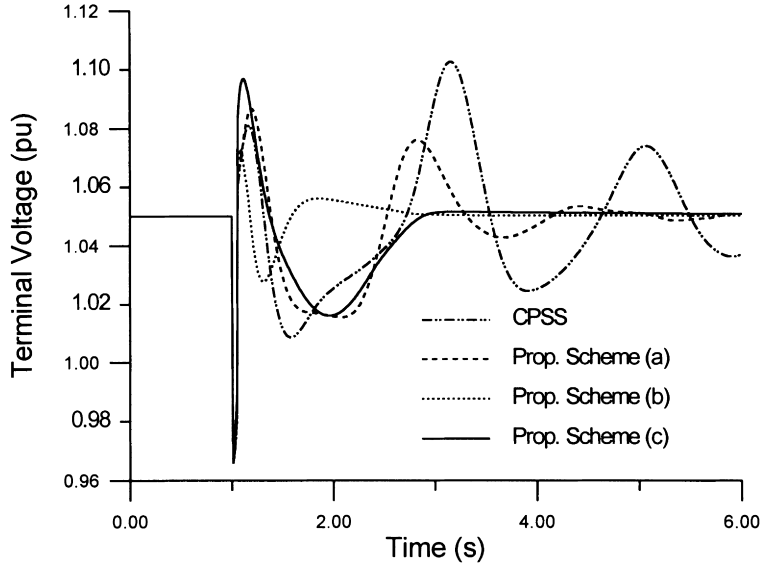

Fig. 13. Terminal voltage response to the fault test with heavy loading.

7. Conclusions

In this study, the effects of PSS and SPS control when applied independently and also through coordinated application has been investigated. The controller design problem is formulated as an optimization problem. Then, SA algorithm has been proposed to search for optimal settings of controller parameters. Different control schemes have been proposed and applied to a weakly connected power system. The proposed schemes were tested under different disturbances, loading conditions, and system parameter variations. The simulation results show that

1. the potential of SA algorithm to solve the problem of PSS and SPS controller design;
2. the SPS controller provides good damping of low frequency oscillations and improves greatly the voltage profile;
3. better damping characteristics can be obtained by coordinated control of PSS and SPS;
4. the effectiveness and robustness of the proposed control schemes over a wide range of loading conditions and system parameter variations.

Acknowledgements

The author acknowledges the support of King Fahd University of Petroleum and Minerals, Saudi Arabia.

Appendix A

Referring to Fig. 1, the voltage $v' = v\angle - \Phi$ and its d and

q components can be written as

$$v'_d = E'_q \sin \Phi - x'_d i_d \sin \Phi + x_q i_q \cos \Phi \quad \text{(A1)}$$

$$v'_q = E'_q \cos \Phi - x'_d i_d \cos \Phi - x_q i_q \sin \Phi \quad \text{(A2)}$$

The load current $i_L = v' Y_L$ and the line current $i_{line} = i - i_L$. The infinite bus voltage $v_b = v' - i_{line} Z$. The components of v_b can be written as

$$v_b \sin \delta = c_1 v'_d - c_2 v'_q - R i_d + X i_q \quad \text{(A3)}$$

$$v_b \cos \delta = c_2 v'_d + c_1 v'_d - X i_d - R i_q \quad \text{(A4)}$$

Substituting from Eqs. (A1) and (A2) into Eqs. (A3) and (A4), the following two equations can be obtained

$$c_5 i_d + c_6 i_q = v_b \sin \delta + c_3 E'_q \quad \text{(A5)}$$

$$c_7 i_d + c_8 i_q = v_b \cos \delta - c_4 E'_q \quad \text{(A6)}$$

Solving Eqs. (A5) and (A6) simultaneously, i_d and i_q expressions can be obtained. Linearizing Eqs. (A5) and (A6) at the nominal loading condition, Δi_d and Δi_q can be expressed in terms of $\Delta\delta$, $\Delta E'_q$ and $\Delta\Phi$ as follows.

$$c_5 \Delta i_d + c_6 \Delta i_q = v_b \cos \delta \Delta\delta + c_3 \Delta E'_q + c_9 \Delta\Phi \quad \text{(A7)}$$

$$c_7 \Delta i_d + c_8 \Delta i_q = -v_b \sin \delta \Delta\delta - c_4 \Delta E'_q + c_{10} \Delta\Phi \quad \text{(A8)}$$

Solving Eqs. (A7) and (A8) simultaneously, Δi_d and Δi_q can be expressed as

$$\Delta i_d = c_{11} \Delta\delta + c_{12} \Delta E'_q + c_{13} \Delta\Phi \quad \text{(A9)}$$

$$\Delta i_q = c_{14} \Delta\delta + c_{15} \Delta E'_q + c_{16} \Delta\Phi \quad \text{(A10)}$$

The constants c_1–c_{16} are expressions of Z, Y_L, x'_d, x_q, i_{d0}, i_{q0}, E'_{q0} and Φ_0.

The linearized form of v_d and v_q can be written as

$$\Delta v_d = x_q \Delta i_q \quad \text{(A11)}$$

$$\Delta v_q = \Delta E'_q - x'_d \Delta i_d \quad \text{(A12)}$$

Using Eqs. (A9)–(A12), the following expressions can be easily obtained

$$\Delta P_e = K_1 \Delta\delta + K_2 \Delta E'_q + K_p \Delta\Phi \quad \text{(A13)}$$

$$(K_3 + sT'_{do}) \Delta E'_q = \Delta E_{fd} - K_4 \Delta\delta - K_q \Delta\Phi \quad \text{(A14)}$$

$$\Delta v = K_5 \Delta\delta + K_6 \Delta E'_q + K_v \Delta\Phi \quad \text{(A15)}$$

where the constants K_1–K_6, K_p, K_q, and K_v are functions of c_{11}–c_{16}.

Appendix B

The system data are as follows:

$M = 9.26$ s; $T'_{do} = 7.76$; $D = 0.0$; $x_d = 0.973$;

$x'_d = 0.19$; $x_q = 0.55$;

$R = -0.034$; $X = 0.997$; $g = 0.249$; $b = 0.262$;

$K_A = 50$; $T_A = 0.05$;

$K_s = 1.0$; $T_s = 0.05$; $|\Phi| \le 10°$; $|u_{PSS}| \le 0.2$ pu;

$|E_{fd}| \le 7.3$ pu.

All resistances and reactances are in pu and time constants are in seconds.

With the nominal loading condition given in Table 2, the system matrices are

$$A = \begin{bmatrix} 0.0 & 377 & 0.0 & 0.0 \\ -0.0588 & 0.0 & -0.1303 & 0.0 \\ -0.0900 & 0.0 & -0.1957 & 0.1289 \\ 95.5320 & 0.0 & -815.93 & -20.00 \end{bmatrix}$$

and

$$B = \begin{bmatrix} 0.0 & 0.0 \\ 0.0 & 0.0775 \\ 0.0 & 0.0185 \\ 1000 & 105.66 \end{bmatrix}$$

References

[1] Yu YN. Electric power system dynamics, New York: Academic Press, 1983.

[2] Anderson PM, Fouad AA. Power system control and stability, Ames, IA: Iowa State University Press, 1977.

[3] deMello FP, Concordia C. Concepts of synchronous machine stability as affected by excitation control. IEEE Trans PAS 1969;88:316–29.

[4] Larsen E, Swann D. Applying power system stabilizers. IEEE Trans PAS 1981;100(6):3017–46.

[5] Tse GT, Tso SK. Refinement of conventional PSS design in multi-machine system by modal analysis. IEEE Trans PWRS 1993;8(2):598–605.

[6] Kundur P, Klein M, Rogers GJ, Zywno MS. Application of power system stabilizers for enhancement of overall system stability. IEEE Trans PWRS 1989;4(2):614–26.

[7] Arredondo JM. Results of a study on location and tuning of power system stabilizers. Int J Electr Power Energy Systems 1997;19(8):563–7.

[8] Lefebvre S. Tuning of stabilizers in multimachine power systems. IEEE Trans PAS 1983;102(2):290–9.

[9] Lim CM, Elangovan S. Design of stabilizers in multimachine power systems. IEE Proc Part C 1985;132(3):146–53.

[10] Osheba SM, Hogg BW. Performance of state space controllers for

turbogenerators in multimachine power systems. IEEE Trans PAS 1982;101(9):3276–83.
[11] Xia D, Heydt GT. Self-tuning controller for generator excitation control. IEEE Trans PAS 1983;102:1877–85.
[12] Samarasinghe V, Pahalawaththa N. Damping of multimodal oscillations in power systems using variable structure control techniques. IEE Proc Genet Transm Distrib 1997;144(3):323–31.
[13] Abido MA, Abdel-Magid YL, Hybridizing rule-based power system stabilizers with genetic algorithms, IEEE PES, Paper # PE-097-PWRS-0-05, 1998.
[14] Park Y, Moon U, Lee K. Self-organizing power system stabilizer using fuzzy auto-regressive moving average (FARMA) model. IEEE Trans Energy Conversion 1996;11(2):442–8.
[15] Rahim A, Nassimi S. Synchronous generator damping enhancement through coordinated control of exciter and SVC. IEE Proc Genet Transm Distrib 1996;143(2):211–8.
[16] Mahran AR, Hogg BW, Al-Sayed ML. Coordinated control of synchronous generator excitation and static var compensator. IEEE Trans Energy Conversion 1992;7(4):615–22.
[17] Wang Y, Hill D, Gao L, Middleton Tr. Stability enhancement and voltage regulation of power systems. IEEE Trans PWRS 1993;8:620–7.
[18] Iravani M, Maratukulam D. Review of semiconductor-controlled (static) phase shifters for power system applications. IEEE Trans PWRS 1994;9(4):1833–9.
[19] Mathur RM, Basati RS. Thyristor controlled static phase shifter for AC power transmission. IEEE Trans PAS 1981;100(5):2650–5.
[20] Baker R, Guth G, Egli W, Eglin O. Control algorithm for a static phase shifting transformer to enhance transient and dynamic stability of large power systems. IEEE Trans PAS 1982;101(9):3532–42.
[21] Sharaf AM, Doraiswami R. Stabilizing an AC link by using static phase shifters. IEEE Trans PAS 1983;102(4):788–96.
[22] Edris A. Enhancement of first-swing stability using a high-speed phase shifter. IEEE Trans PWRS 1991;6(3):1113–8.
[23] wang L. Comparative study of damping schemes on damping generator oscillations. IEEE Trans PWRS 1993;8(2):613–9.
[24] Jiang F, Choi SS, Shrestha G. Power system stability enhancement using static phase shifter. IEEE Trans PWRS 1997;12(1):207–14.
[25] Tan YL, Wang Y. Nonlinear excitation and phase shifter controller for transient stability enhancement of power systems using adaptive control law. Int J Electr Power Energy Systems 1996;18(6):397–403.
[26] Wang HF, Swift FJ, Li M. Analysis of thyristor-controlled phase shifter applied in damping power system oscillations. Int J Electr Power Energy Systems 1997;19(1):1–9.
[27] Fang YJ, Macdonald DC. Dynamic quadrature booster as an aid to system stability. IEE Proc Genet Transm Distrib 1998;145(1):41–47.
[28] Maslennikov VA, Ustinov SM, The optimization method for coordinated tuning of power system regulators, Proceedings of the 12th Power System Computation Conference PSCC, Dresden, 1996, p. 70–5.
[29] Aarts E, Korst J. Simulated annealing and Boltzmann machines: a stochastic approach to combinatorial optimization and neural computing, New York: Wiley, 1989.
[30] Metropolis N, Rosenbluth A, Rosenbluth M, Teller A, Teller E. Equation of state calculations by fast computing machines. J Chem Phys 1953;21:1087–92.
[31] Xing K, Kusic G. Application of thyristor-controlled phase shifters to minimize real power losses and augment stability of power systems. IEEE Trans Energy Conversion 1988;3(4):792–8.
[32] Hsu YY, Chen CL. Identification of optimum location for stabilizer applications using participation factors. IEE Proc Part C 1987;134(3):238–44.